

Steady-state Operation of Very Long EHV AC Cable Lines

L. Colla, F. M. Gatta, A. Geri, S. Lauria, *Member, IEEE*, and M. Maccioni

Abstract—Technical improvements in the construction of EHV cables have made possible the installation of very long EHV AC cable lines; with a sufficient degree of voltage control such lines can retain a large part of their theoretical power transmission capability. Quick, accurate expressions for the evaluation of cable length-loading relationships are given to that purpose. Appropriate choice of shunt compensation by standard, fixed-type shunt reactors, aimed at solving most steady-state constraints on the operation of very long EHV cable lines as well as temporary overvoltages, is discussed. Analysis of the operating envelopes of very long EHV AC cable lines shows that line losses play a very limited role. A simple criterion for optimal utilization of real, lossy cable lines is also proposed.

Index Terms— Cable ampacity, capacitive switching, EHV cables, mixed lines, shunt compensation, temporary overvoltages, voltage and reactive power control.

I. INTRODUCTION

INFRASTRUCTURAL congestion and public opposition are causing an increased recourse to EHV AC underground cable lines (CLs), up to 550 kV [1]. Modern underground HV/EHV AC cables almost always use cross-linked polyethylene (XLPE) insulation. These cables enjoy several advantages in comparison with previously used fluid-filled (FF) cables, especially in terms of installation, maintenance and weight.

In the EHV ac submarine cable field, the switch from FF to XLPE cables has not yet taken place; however, prompted by the ongoing installation of large offshore wind farms (e.g. 400-500 MW), three-core XLPE-insulated HV AC submarine cables up to 245 kV are now available, with 400 kV single-core cables undergoing tests [2].

The operating envelope of EHV AC cable lines (CLs) is still dictated by their relatively low ampacity, compounded for long CLs by the derating effect of the cable's own charging current. Some of the benefits accrued by the use of XLPE insulation, such as the smaller shunt capacitance and the higher ampacity (due to slightly higher operating temperatures and lower dielectric losses), yield wider operating limits with respect to FF cables. Considering steady-state constraints, it is possible to operate underground EHV CLs longer than 100 km

without intermediate compensating stations.

The present paper deals with the steady state operation of long HV/EHV AC CLs, and their inductive shunt compensation, aiming at pointing out the operating envelope of very long (say, 100 km or more) HV/EHV AC cables and some of the attendant technical requirements, challenges and possible solutions. Although the choice of such long CLs could be questioned at the very least on the grounds of cost, any evaluation must take into account the widespread opposition to overhead lines (OHLs) construction.

The paper is organized as follows: maximum length/utilization is discussed in Section II, for lossless cable lines. Shunt compensation design criteria and calculations are reported in Section III, while the actual operating envelope of lossy cables cable is treated in Section IV. Section V discusses several issues regarding the integration of long CLs in the transmission network.

II. MAXIMUM LENGTH OF EHV AC CLS

A. Lossless analysis – optimal operation and maximum length

As anticipated in the Introduction, cable loading by their own charging current is the main issue of long AC CLs at EHV level: constraints on steady-state operation of EHV AC CLs are still those outlined in two classic papers of 1956 and 1962 [3][4], despite the significant changes in cable technology occurred in the last 50 years.

Compared to OHLs, the shunt capacitance of XLPE-insulated CLs, p.u. of length, is 15-20 times larger whereas the ratio of positive-sequence series reactances is in the 0.5÷1 range, so that the surge impedance loading (SIL) of CLs is several times greater than that of OHLs. Usually such SIL far exceeds the cable ampacity, which (without forced cooling) is invariably lower than the thermal limit current of OHLs.

As a consequence, HV/EHV AC CLs are current-limited and have a significant reactive power surplus in any operating condition: the associated charging current increases with CL length, up to and beyond cable ampacity.

Table I reports positive-sequence line electrical data and ampacity of several single-circuit EHV AC CLs, using single-core XLPE-insulated cables. Entries 1, 3 and 4 in Table I are underground cables, in direct-buried, flat laying with cross-bonded sheaths. Cable 2 data refer to an hypothetical 1400 mm² submarine cable, and are largely based (except for the capacitance) on the new Sicily-Italy 400 kV-50 Hz link. Submarine cables have smaller conductors than underground cables, for mechanical reasons; for a given conductor cross-

F. M. Gatta, A. Geri, S. Lauria and M. Maccioni are with the Department of Electrical Engineering, University of Rome "Sapienza", 00184 Roma, Italia (e-mail: fabiomassimo.gatta@uniroma1.it; alberto.geri@uniroma1.it; stefano.lauria@uniroma1.it; marco.maccioni@uniroma1.it).

L. Colla is with TERN S.p.A, via Ostiense 92, 00154 Roma, Italia (e-mail: luigi.colla@terna.it).

section their equivalent positive sequence resistance is also higher due to solid bonding of sheath and armour.

TABLE I
EHV CABLE DATA

Cable	U_n [kV]	f_n [Hz]	S [mm ²]	r_1+jx_1 [Ω/km]	c_1 [nF/km]	SIL [MVA]	I_z [A]	S_z [MVA]
1	400	50	2500	0.0133+j0.172	234	3308	1788	1239
2			1400	0.026+j0.080	195	4430	1500	1039
3	345	60	1520	0.017+j0.200	175	2162	1550	926
4	525		2500	0.0137+j0.217	209	5252	1600	1455

(see text for details)

Table I clearly shows that SIL of CLs is a multiple of the apparent power deliverable at thermal limit, S_z ; even when loaded at ampacity, modern XLPE-insulated CLs with large conductors, such as cables 1 and 4 in Table I, thus have a large reactive power surplus, about 10 Mvar/km for the 400kV-50 Hz cable and 20 Mvar/km for the 525kV-60 Hz cable. To obtain the best possible utilization of the CL, it is necessary to evacuate the same amount of reactive power at both terminals [4], provided that the network there is able to exchange reactive power with the CL (to an amount which is limited in practice by inductive shunt compensation).

In the lossless case, the condition on symmetrical reactive power output translates into equality of the terminal voltages (see the Appendix). Under the above hypothesis the maximum operable length at thermal limit, MCLTL (km) of a cable without intermediate compensation for a given active power flow P is [5]:

$$MCLTL = \frac{1}{K''} \arctg \left[\frac{2 P_c S_z \sqrt{1 - \rho^2}}{P_c^2 - S_z^2} \right] \quad (1)$$

where P_c (MW) and S_z (MVA) are respectively the SIL and the apparent power at ampacity I_z , calculated for the chosen voltage U (f.i. the nominal system voltage U_n or the maximum system operation voltage U_s); $\rho = P/S_z$ is the p.u. cable utilization and K'' (km⁻¹) is the CL propagation constant. Derivation of (1) and following is reported in the Appendix.

The theoretical maximum length L_{Max} of a CL without intermediate compensating stations is given by (1) in the limit case of nil real power transmission $\rho=0$.

$$L_{Max} = \frac{1}{K''} \cdot \arctg \left(\frac{2 P_c S_z}{P_c^2 - S_z^2} \right) \quad (2)$$

For $L=L_{Max}$ and equal terminal voltages, the CL is fully loaded at both ends by its charging current only. It can be shown that L_{Max} is twice the length L_{Crit} for which the charging current (in no-load radial operation with the same impressed voltage U used in (1)), equals the cable ampacity:

$$L_{Max} = \frac{2}{K''} \cdot \arctg \left(\frac{\sqrt{3} \cdot Z_c I_z}{U} \right) = 2 \cdot L_{Crit} \quad (3)$$

where Z_c is the cable surge impedance (Ω), I_z is the ampacity (kA) and U is the operating voltage (kV). A good practical approximation of L_{Crit} is given by the ratio between I_z and charging current p.u. of length.

Fig. 1 shows qualitative plots of voltage, reactive power

and active power along a lossless CL operated with equal terminal voltages.

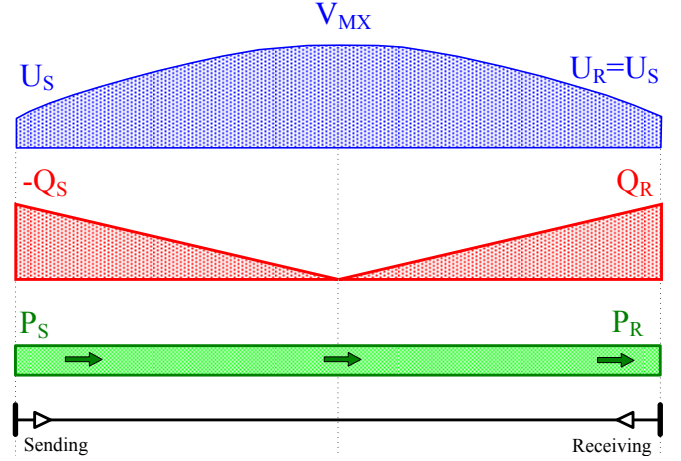


Fig. 1. Voltage profile, reactive and active power flows over a lossless EHV cable line operated with equal terminal voltages.

Open-ended steady-state operation of cables longer than L_{Crit} is only possible (up to L_{Max}) with inductive shunt compensation at the open receiving end (see f.i. [4]).

Given the length L and terminal voltage U , (1) can be solved for ρ . Multiplying by S_z , the maximum transmitted power of the lossless, uninterrupted CL is arrived at:

$$P_{Max} = S_z \cdot \sqrt{1 - \left[\frac{P_c^2 - S_z^2}{2 P_c S_z} \cdot \text{tg}(K''L) \right]^2} \quad (4)$$

Table II shows values of L_{Max} and ρ_{Max}/P_{Max} calculated for $L=0.7 \cdot L_{Max}$. The latter value roughly defines a “crossover” length, with an attendant P_{Max} around $0.75 \cdot S_z$. The latter is practically independent from terminal voltage, varying less than 1% in the whole admissible voltage range.

TABLE II
MAXIMUM CL LENGTH AND UTILISATION FOR $L=0.7 \cdot L_{Max}$

	$U_S=U_R$ [kV]	L_{Max} [km]	$(0.7 \cdot L_{Max})$		
			L [km]	P_{Max} [MW]	ρ [p.u.]
Cable 1	400	201.5	141.1	962.3	0.78
Cable 2	400	207.2	145.1	768.2	0.74
Cable 3	345	222.9	156.0	736.6	0.80
Cable 4	525	130.7	91.5	1090.0	0.75

(all values calculated at $U=U_n$)

Cables longer than $0.7 \cdot L_{Max}$ would be actually able to transmit more power with lower terminal voltages (e.g., 380 kV instead of 400 kV) in contradiction to the current operating practice of EHV transmission networks, with voltages close to the maximum system voltage. However, P_{Max} sharply decreases for such cable lengths. In Fig. 2, values of ρ_{max} and P_{Max} for cables in Table I are plotted versus cable length; three curves, corresponding to different operating voltages, are reported for each cable.

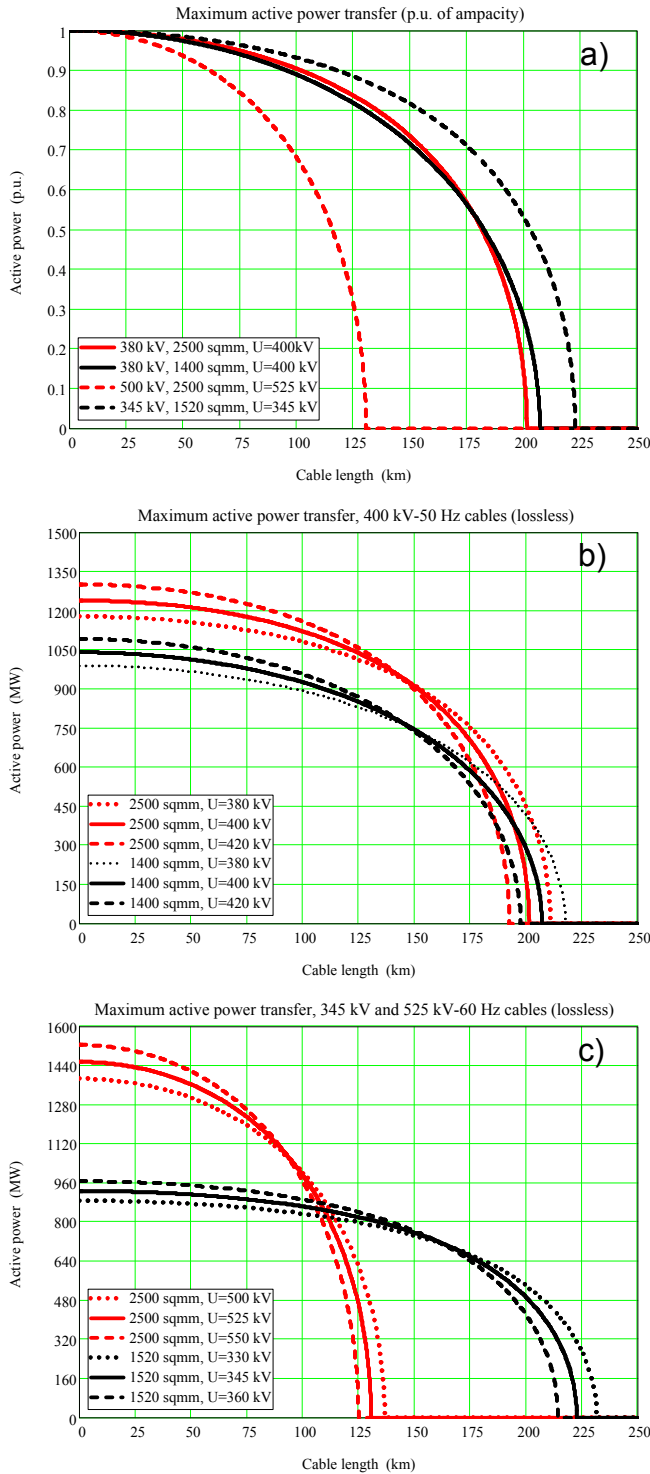


Fig. 2. Maximum transmissible active power at thermal limit, vs. length. Equal terminal voltages, losses neglected, cable data from Table I. a) cable utilization; b) 400 kV-50 Hz CLs; c) 345 kV and 500 kV-60 Hz CLs.

B. Lossless analysis - Non-optimal operation

If the terminal voltages of the lossless CL differ, the reactive power profile along the line becomes asymmetrical, with more power flowing toward the terminal at lower voltage. Due to the uneven loading of the CL, the maximum active power transmission decreases with respect to the limit calculated with (1) for the highest of the two terminal voltages. Steady-state CL operating envelopes can be obtained

by enforcing the ampacity constraint on the current (at either end of the CL) in the single-phase transmission line equations [3], obtaining a number of capability curves, f.i. the lens-shaped sectors in (P,Q) plane of [6][7].

Useful information about the CL operating envelope is conveyed by curves depicting the maximum power at thermal limit P_{Max} as a function of one of the terminal voltages, with the other kept constant: the curves consist of branches pertaining to the sending-end and receiving-end current limits, which enclose the operating area of the CL. Branches intersect at $U_R=U_S$, where the maximum transmissible power defined by (1) is found.

Fig. 3 shows lossless curves of P_{Max} versus receiving-end voltage U_R , with the sending-end voltage U_S kept at the nominal value, for cables 1 and 4 in Table I (400kV-50 Hz and 525 kV-60 Hz, 2500 mm² underground cables). Three different CL lengths are considered for each cable, approximately equal to 25%, 50% and 75% of the relevant L_{Max} at rated voltage, reported in Table II. Such lengths amount to 50 km, 100 km and 150 km for Cable 1 and respectively 32.2 km, 64.4 km and 96.6 km for Cable 4.

Operating envelopes for the 400 kV-50 Hz cables encompass all the (380, 420) kV range, whereas 525 kV-60 Hz cables can not operate permanently beyond certain values of the receiving-end voltage. Moreover, both in Fig. 3a and 3b shorter cables apparently have narrower operating areas than longer ones, due to the fact that the same terminal voltage difference drives a larger reactive power flow along the shorter cable. It is however quite unlikely that such largely different voltages appear at the CL terminal nodes, which are quite ‘close’ electrically. In that case, the ensuing reactive power flows would have a self-stabilising effect, raising the voltage at the depressed terminal and lowering it at the strong one. Problems could arise if the voltages of the terminal nodes were tightly regulated, e.g. by nearby synchronous generators, in terms of CL overload and generator under/overexcitation.

III. SHUNT COMPENSATION AND REACTIVE POWER BALANCE

A. Sizing criteria for shunt reactors

Unless the long CLs are adequately shunt compensated, their significant reactive power output may cause local voltage rises as well as excessive underexcitation of the nearest synchronous generators. In case of no-load energization and load rejection, high temporary overvoltages (TOVs) can occur; the large no-load charging current of long uncompensated EHV AC cables can easily exceed the rated line-charging breaking current of circuit breakers (CBs). All these problems can be reduced or eliminated by installing shunt reactors (SRs) connected to the cable ends.

Shunt compensation design criteria related to the no-load, open-ended operation of long mixed overhead-cable lines were discussed in [8][9]. For the homogeneous lines treated here, algorithms A and B of [9] reduce to simpler expressions, easily obtainable f.i. from quick TOV evaluation formulas given in [10].

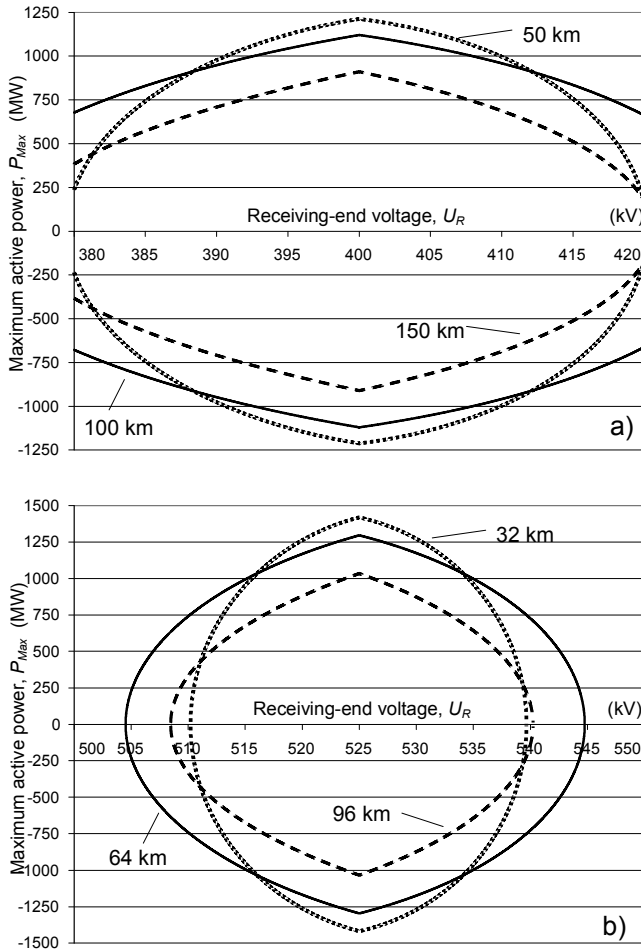


Fig. 3. Power transmission at thermal limit, vs. receiving-end voltage U_R . Losses neglected, 2500 mm² underground cable data from Table I. a) Cable 1, sending-end voltage $U_S=400$ kV; b) Cable 4, sending-end voltage $U_S=525$ kV.

SR dimensioning criteria considered in [9] were:

- Voltage “jump” at the supply node.** Sudden voltage changes due to routine manoeuvres like CL no-load energization or disconnection should be limited, in order to reduce the disturbance to customers. The step voltage change at the supply node upon energization or disconnection is also a good approximation of the reactive power injected by the CL into the supply network, in p.u. of the available short-circuit power.
- Receiving (open) end overvoltages.** The TOV at the open end of the CL or mixed line, following the no-load energization or load rejection, must be contained in order to allow line reclosure (slow speed automatic and manual) as well as to avoid damage to line-connected apparatuses. The TOV capability of metal oxide surge arresters (MOSAs) protecting SRs and cables must be checked, particularly in case of load rejection with heavy power flows. In case of occurrence of large TOVs, line fast switching-off at the energizing end via transfer tripping is a remedy, provided that CBs have sufficient charging current breaking capacity.
- Rated line-charging breaking current of line CBs.** Use of a high shunt compensation with SRs permanently connected to the CL ends, warrants that the capacitive current to be

interrupted when switching-off the CL is in all cases lower than the rated line/cable charging current breaking capability. The line-charging breaking current constraint must be enforced for credible sending-end TOV values, such as those due to load rejections and/or ground faults. SRs also ensure that the TOVs have generally a small amplitude.

- Sending-end CL current.** For CLs longer than the L_{Crit} of (3), shunt compensation must ensure that cable sending-end current (downstream of SRs) stays below ampacity.

B. Application to long CLs

Fig. 4 shows shunt compensation requirements, calculated under constraints listed in Sec. III-A, of the already examined 50 km, 100 km and 150 km long 400kV-50Hz CLs (cable 1 in Table I). The shunt compensation degree K_{Sh} and the rated SR power to be installed at each line end Q_{SR} (50% of total) are plotted as a function of the supply node short-circuit power.

The assumed design limit of the supply bus voltage step change is $\Delta U=3\%$, with results obtained for $\Delta U=2\%$ and 4% also being reported. At the open receiving end of the line, 1.1 p.u. TOVs have been considered having in mind Class 4 MOSAs commonly installed in the Italian 400 kV-50 Hz transmission network [11], with maximum continuous operating voltage $U_c=265$ kV. Line-charging breaking current constraints consider internationally standardized rated values for 420 kV and 550 kV CBs, i.e. 400 A and 500 A rms [12][13] with 1.4 p.u. pre-switching voltage to account for the possible breaking in presence of a 1- Φ -to-Gr or a Φ - Φ -to-Gr fault in the CL. Sending-end cable current equal to I_z was also considered for the 150 km long CL.

Results consistently follow the pattern outlined in [9]. Step voltage change for routine switching (constraint A) rules at weak supply nodes, with values of K_{Sh} between 80 and 96% depending on CL length. Rated cable-charging breaking current (constraint C) takes over when short-circuit power increases beyond (5÷10) GVA, depending on ratings: attendant values of K_{Sh} range between 70% and 92%. Receiving-end overvoltage (constraint B) and cable ampacity (constraint D) are never decisive for the simulated CLs due to the limited Ferranti voltage rise along the CL, even for CL lengths around $0.75 \cdot L_{Max}$.

If line energization and dropping were only performed at the most powerful terminal (“best-end switching”), SRs could be sized according to the line-charging breaking current criterion. Under this regard, further savings on SRs could be envisaged with the adoption of higher-rated CBs or uprating existing ones in view of the low first-phase factor and favourable TRV waveshape of compensated CLs.

However, since operation at low values of short circuit power and/or limited generators’ underexcitation capability can not be ruled out, it is probably advisable to size SRs based on the more stringent criteria of sending-end step voltage unless additional switchable busbar-connected reactors are available at the interested substation.

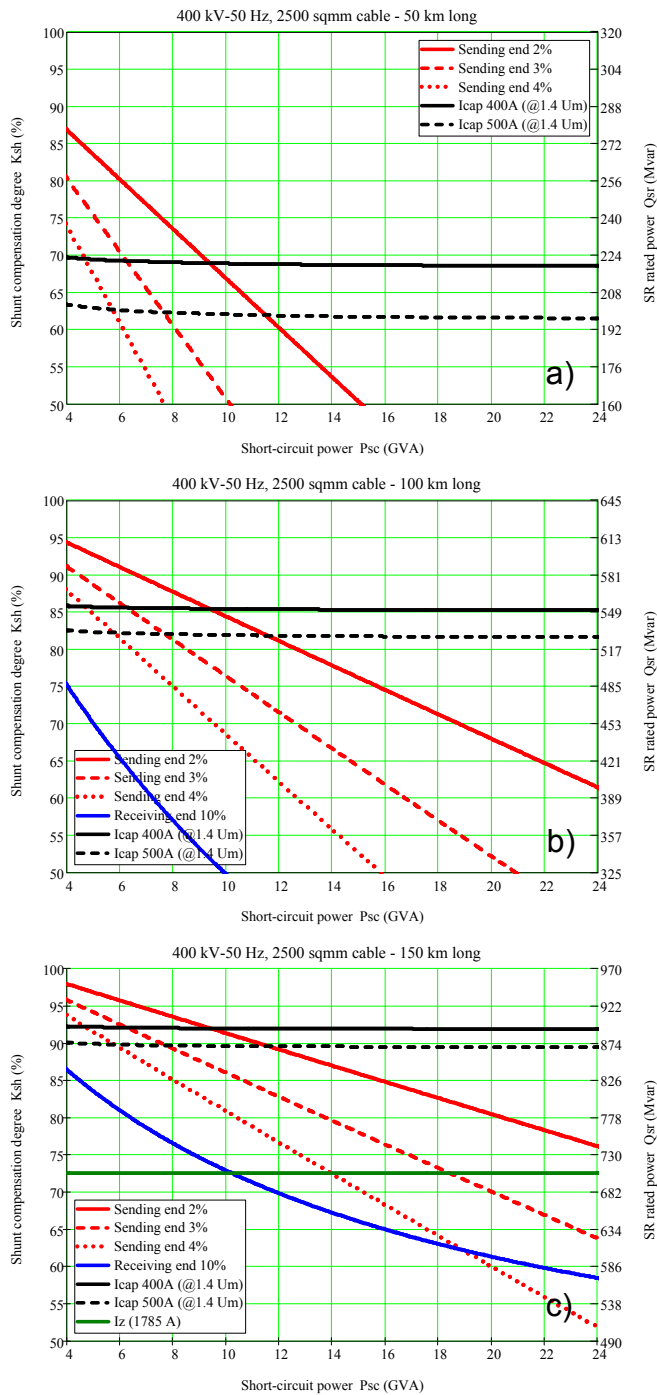


Fig. 4. Shunt compensation requirements of 400 kV-50 Hz CLs (Cable 1 of Table I) of different lengths. Total 420 kV SRs power, Q_{SR} and shunt compensation degree, K_{Sh} vs. short circuit power at supply node, P_{sc} . a) 50 km CL, b) 100 km CL, c) 150 km CL.

Fig. 5 depicts the results of similar shunt compensation calculations, carried out for three different lengths of 500kV-60Hz CL (cable 4 in Table I), namely 32.2 km, 64.4 km, and 96.6 km. Plots closely follow those in Fig. 4, with values of K_{Sh} for ruling criteria differing less than 2% from those previously found.

In conclusion, shunt compensation values selected for further simulation are those found under constraint A ($\Delta U=3\%$ at sending end), for $P_{sc}=4000$ MVA, and listed in Table III.

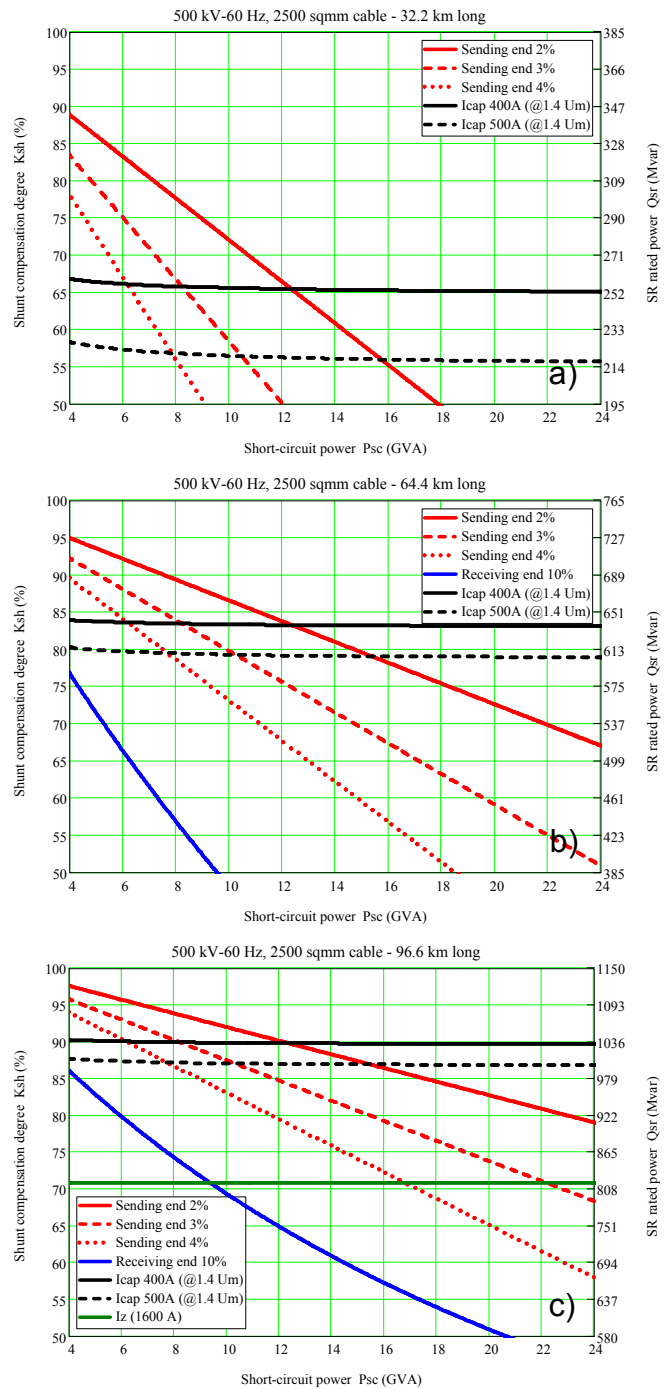


Fig. 5. Shunt compensation requirements of 500 kV-60 Hz CLs (Cable 4 of Table I) of different lengths. Total 550 kV SRs power, Q_{SR} and shunt compensation degree, K_{Sh} vs. short circuit power at supply node, P_{sc} . a) 32.2 km CL, b) 64.4 km CL, c) 96.6 km CL.

TABLE III
SHUNT COMPENSATION VALUES SELECTED FOR THE SIMULATED CLS

Cable 1 (400 kV- 50 Hz)	L [km]	50	100	150	
	$2 \times Q_{SR}$ [Mvar]		2×260	2×590	2×930
K_{Sh} [%]		80.2	91.0	95.6	
Cable 4 (500 kV- 60 Hz)	L [km]	32.2	64.4	96.6	
	$2 \times Q_{SR}$ [Mvar]		2×320	2×710	2×1100
	K_{Sh} [%]		83.4	92.5	95.6

(Q_{SR} values calculated at 420 kV and 550 kV, respectively)

IV. OPERATING ENVELOPES OF LOSSY CLS

Actual operating envelopes must take into account losses, including those in SRs. Fig. 6 shows (U_R, P_R) curves for previously considered cables, with losses considered (shunt compensation from Table III, with quality factor $Q=400$). P_{Max} now refers to the active power delivered at the receiving end of the CL all other conditions are equal to those of Fig. 3.

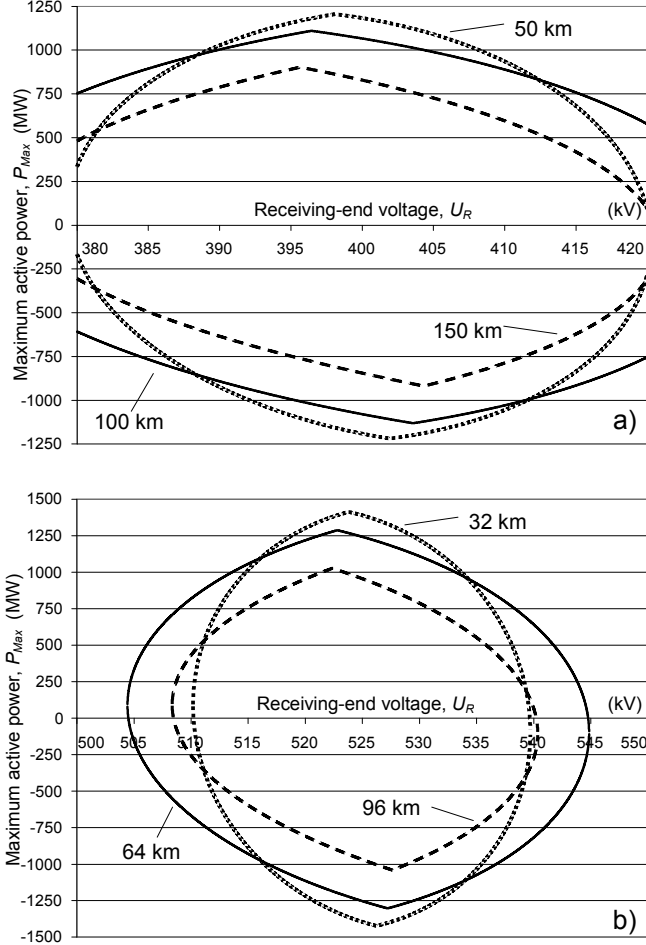


Fig. 6. Same as Fig. 3, with losses included. Power transmission at thermal limit, vs. receiving-end voltage U_R . 2500 mm² underground cable data from Table I. a) Cable 1, sending-end voltage $U_S=400$ kV; b) Cable 4, sending-end voltage $U_S=525$ kV.

On an equal sending-end voltage basis the reduction in transmissible power brought about by losses is very small as shown in Table IV, i.e. under 1%.

TABLE IV
IMPACT OF LOSSES ON MAXIMUM POWER TRANSMISSION

	L [km]	P_{Max}				Losses [%]
		Lossless		Lossy [MW]	Δ [%]	
		[MW]	ρ			
Cable 1 $U_S=400$ kV	50	1212.1	0.98	1205.7	0.53	0.62
	100	1120.6	0.90	1110.1	0.94	1.26
	150	910.8	0.74	902.5	0.98	1.96
Cable 4 $U_S=525$ kV	32.2	1418.2	0.97	1414.1	0.29	0.37
	64.4	1295.9	0.89	1289.0	0.53	0.78
	96.6	1034.1	0.71	1027.8	0.61	1.28

The main difference between (U_R, P_R) curves of Fig. 3 and Fig. 6 is that in the latter maxima of transmitted power are found for receiving-end voltage values U_R smaller than U_S . “Lossy” (U_R, P_R) operating envelopes in Fig. 6 are thus distorted in comparison to the lossless ones of Fig. 3.

At the point of maximum delivered power, the current and reactive power profile flows along the lossy CL is practically symmetrical, just as in the lossless case: this can be appreciated in Fig. 7, which refers to the maximum power transfer of the 150 km long “lossy” CL (Cable 1) with $U_S=400$ kV (third row of Table IV)

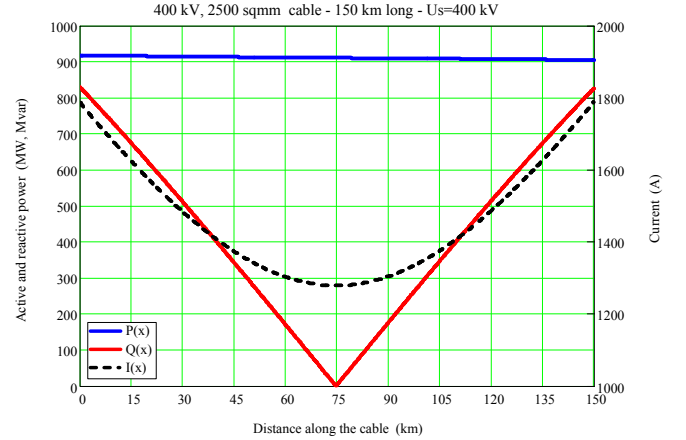


Fig. 7. Current, active power and reactive power flows along 400 kV-50 Hz, 150 km long CL (cable 1 in Table I, losses included). Maximum power transfer (see Table IV) with sending-end voltage $U_S=400$ kV and receiving-end voltage $U_R=395.63$ kV.

The overall ‘reactive’ voltage drop is thus practically nil and the difference between sending-end and receiving-end voltage, due to active power flowing along the cable series resistance of the cable R_C , can be evaluated by means of the first-order approximation:

$$\Delta U_{SR,opt} = \frac{R_C \cdot P_R}{U_R} \quad (5)$$

Compliance with (5) implicitly defines a symmetrical reactive power profile, hence optimal CL operation for a given (P_R, U_R) couple of values: mismatches between (5) and simulated values of $\Delta U_{SR,opt}$ are generally under 2%. For the case depicted in Fig. 7, U_R is 395.63 kV: the actual voltage difference ΔU_{SR} differs from (5) by less than 1.4%.

In practice, due to the non-uniform current flow (Fig. 7), temperature and resistance might vary along the CL, and the temperature profile could be generally unsymmetrical; modern real time thermal rating (RTTR) systems allow a precise estimation of the overall resistive drop along the CL, hence a satisfactory application of (5).

V. THE EXTRA-LONG EHV CABLE IN THE NETWORK

Integration of long cables in the EHV AC transmission network [14] raises many issues. Among these:

- A CL has a smaller positive-sequence series reactance than an OHL of equal length, especially for the closely spaced arrangements of the cable line which are usually adopted

(to reduce magnetic fields, right-of-ways and costs of excavation). This can make the cable a preferential path for active power flows.

- In order reproduce the optimal operating condition of Sec. III, i.e. fully exploit the cable ampacity, a certain degree of control over terminal voltages is desirable.

The first problem requires careful system studies when the cable is put in parallel with an existing single-circuit overhead line and, generally, when it connects two buses previously characterized by a large standing phase angle difference.

Strategically placed phase shifting transformers (PSTs) could solve the problem although at a cost and with possible repercussion on $N-1$ security in case of PST outage. Other alternatives are the reduction of the transfer reactance of “parallel” overhead transmission paths by installing series capacitors (effective but expensive) or, tentatively, the dual measure of increasing the cable reactance by means of series reactors at the cable terminals [1].

Typical CL and OHL impedances and feasible EHV cable lengths, dictate relatively small (low ohmic impedance) series reactors, with very severe short-circuit withstand requirements. Moreover, series reactors installed between station busbars and SRs, would worsen the CL behaviour at no-load by reducing the short-circuit power “seen” by the CL; if installed between SRs and cable, they would also reduce the effectiveness of SRs and raise cable voltages.

Adjustable (tapped winding) SRs can be used to control CL terminal voltages and reactive power profiles [5]. When applied to a long mixed line, the simple control procedure proposed in [5] required large reactive power changes (up to the disconnection of one or more SRs), thus violating operational security constraints on minimum shunt compensation listed in Sec. III. However, for a CL the required voltage control range should be quite smaller, and reactors at either end of the CL could be adjusted in opposite directions around an intermediate setpoint.

VI. CONCLUSIONS

Maximum length and power transmission capability of modern, XLPE-insulated EHV AC cables are mostly dictated by cable ampacity and derating due to charging current.

- Lossless analysis allows quick and accurate closed-form evaluation of length/loading limits. Considering the largest cables commercially available, such analyses show theoretical maximum (zero-transmission) uninterrupted lengths around 200 km at 400 kV-60 Hz and 130 km at 500 kV-60 Hz. At 75% of those lengths, cable lines still retain over 70% of their ampacity for active power transmission.
- Operation of long EHV AC cables requires a high degree of inductive shunt compensation, reaching over 95% for the longest mentioned CLs. Such reactor ratings are dictated by routine switching voltage step change with low network short circuit power. Even in very strong networks, however, rated cable-charging breaking current of line circuit breakers dictates an high minimum compensation degree (over 90% for the longest cables).

- Optimal exploitation of cable lines, both lossless and real, requires symmetrical reactive power profiles along the cable. In lossy cables, that can be achieved simply by enforcing that the difference between terminal voltages is approximately equal to the “resistive”, first-order approximation voltage drop along the cable for a given transmitted power.
- For the modern, low-loss EHV AC cables taken into account, calculated values of maximum active power transmission closely mirror those obtained by simplified lossless analysis.

VII. APPENDIX

Along a lossless CL, the active power flow is constant; the optimal operating condition is attained when the reactive power surplus is equally shared between the line terminals. The attendant maximum active power transfer at thermal limit is reached when the current at both terminal equals ampacity. Analytically, the condition can be expressed as:

$$\begin{cases} P_S = P_R = \frac{U_S U_R}{B} \sin \vartheta = \rho \cdot S_z \\ Q_S = -Q_R = \frac{A U_S^2}{B} - \frac{U_S U_R}{B} \cos \vartheta = -\sqrt{1 - \rho^2} \cdot S_z \\ Q_R = \frac{U_S U_R}{B} \cos \vartheta - \frac{A U_R^2}{B} = \sqrt{1 - \rho^2} \cdot S_z \end{cases} \quad (6)$$

Subscripts ‘S’ and ‘R’ stand for sending- and receiving-end, respectively; A and B are the magnitudes of the attendant transmission constants, θ is the phase shift between terminal voltages and S_z is the apparent power at ampacity for a given voltage U. The reactive power relationship ($Q_S = -Q_R$) yields:

$$U_S = U_R \quad (7)$$

Taking $U_S = U_R = U$, (6) reduces to:

$$\begin{cases} \frac{U^2}{B} \sin \vartheta = \rho \cdot S_z \\ \frac{U^2}{B} - \frac{A U^2}{B} \cos \vartheta = \sqrt{1 - \rho^2} \cdot S_z \end{cases} \quad (8)$$

Squaring and summing (8),

$$\begin{cases} S_z^2 = \frac{U^4(1 + A^2)}{B^2} - \frac{2A U^4}{B^2} \cos \vartheta \\ \frac{U^2}{B} - \frac{A U^2}{B} \cos \vartheta = \sqrt{1 - \rho^2} \cdot S_z \end{cases} \quad (9)$$

Lastly, eliminating θ ,

$$\frac{U^4 \cdot (1 - A^2)}{B^2} - S_z^2 = \frac{2A U^2}{B} \sqrt{1 - \rho^2} \cdot S_z \quad (10)$$

Remembering the lossless expressions $A = \cos(k'' \cdot L)$, $B = Z_c \cdot \sin(k'' \cdot L)$, with k'' propagation constant, L line length, Z_c surge impedance, as well as the surge impedance loading $P_c = U^2 / Z_c$ the final expression is arrived at:

$$\frac{P_c^2 - S_z^2}{2P_c S_z} \tan(k'' \cdot L) = \sqrt{1 - \rho^2} \quad (11)$$

VIII. REFERENCES

- [1] CIGRE Working Group B1.07, "Statistics of AC underground cables in power networks," CIGRE Brochure 338, December 2007.
- [2] G. Evenset, J. E. Larsen, B. Knutsen, and K. Faugstad, "Qualification, supply and installation of the world's first 420 kV XLPE submarine cable system in Norway," in *Proc. Jicable '07 Conf.*, Paper A-93.
- [3] C. S. Schiffreen, and W. C. Marble, "Charging current limitations in operation of high-voltage cable lines," *AIEE Trans. pt. III (Power Apparatus and Systems)*, vol. 75, pp. 803-817, Oct. 1956.
- [4] C. S. Schiffreen, and J. J. Dougherty, "Long cable lines – alternating current with reactor compensation or direct current," *IEEE Trans. Power Apparatus and Systems*, vol. 81, pp. 169-178, June 1962.
- [5] F. M. Gatta, and S. Lauria, "Very long EHV cables and mixed overhead-cable lines. Steady-state operation," in *Proc. 2005 IEEE St. Petersburg Power Tech Conf.*, Paper n. 297.
- [6] R. Benato, and A. Paolucci, "Operating capability of long AC EHV transmission cables," *Electric Power Systems Research*, vol. 75 n.1, pp. 17-27, July 2005.
- [7] M. Márquez and G. Alvarez, "Active and reactive operation area of insulated cables," in *Proc. CIGRE General Session 2008*, Paper B1-310
- [8] S. Lauria, F. M. Gatta, and L. Colla, "Dimensionamento della compensazione derivata nelle linee AAT 'miste' cavo-aerea," (in Italian), in *Proc. 101st AEI meeting*, Capri (Italy) 16-20 Sept. 2006
- [9] S. Lauria, F. M. Gatta, and L. Colla, "Shunt compensation of EHV Cables and Mixed Overhead-Cable Lines," in *Proc. 2007 IEEE Lausanne Power Tech Conf.*, Paper n. 562.
- [10] CIGRE WG 33-06 "Metal oxide surge arresters in AC systems – Part 3," *ELECTRA* n° 128, January 1990
- [11] TERNA (2006, Oct.). Requisiti e caratteristiche di riferimento delle stazioni elettriche della RTN (in Italian), Annex A3 to the Network Code, Rev. 01. TERNA S.p.A: Rome, Italy. [Online]. Available: http://www.terna.it/default/Home/SISTEMA_ELETTTRICO/codice_rete/tabid/106/Default.aspx
- [12] *High-voltage alternating-current circuit-breakers*, IEC Standard 62271-100, May 2001.
- [13] *AC high-voltage circuit breakers rated on a symmetrical current basis - Preferred ratings and related required capabilities*, ANSI Standard C37.06-2000, May 2000.
- [14] CIGRE Working Group B1.19, "General guidelines for the integration of a new underground cable system in the network," CIGRE Brochure 250, August 2004.

Luigi Colla was born in Marino, Italy, in 1980. He received the master degree and the Ph.D. in electrical engineering from the University of Rome "La Sapienza" in 2004 and in 2007, respectively. In 2007 he joined the Planning and Grid Development Department of Terna, Italian TSO. His main research interests are in power systems analysis, HVAC and HVDC transmission, electromagnetic transients and long distance transmission.

Fabio Massimo Gatta was born in Alatri (Italy) in 1956. In 1981 he received a doctor degree in Electrical Engineering from Rome University (Hons). He then joined the Rome University's Department of Electrical Engineering where he was appointed Researcher and in 1998 appointed Associate Professor in Electrical Power Systems. His main research interests are in the field of power system analysis, long distance transmission, transient stability, temporary and transient overvoltages, series and shunt compensation, SSR, distributed generation, power plants, design, planning and operation of transmission and distribution network, unconventional distribution systems

Alberto Geri was born in Terni (Italy) on August 4, 1961. He received a University degree in Electrical Engineering from University of Rome "La Sapienza" in 1987. He began academic activity in 1989 as researcher of Electrical Science at University of Rome "La Sapienza" and from 2000 he is Associate Professor in Electrical Engineering at the same university. He has been the recipient of many research contracts and grants from institutional sources as well as private investors. He began research activity in 1982 and his interests include MHD energy conversion, low frequency electric and magnetic field computation, high frequency magnetic device modelization and non-linear electromagnetic problems related to lightning protection systems and grounding systems. These activities have been documented by more than ninety papers presented at international conferences or published in peer-reviewed international journals.

Stefano Lauria (M'1998) was born in Rome (Italy) in 1969. He received the Master degree and the Ph.D. in electrical engineering from the University of Rome "La Sapienza" in 1996 and in 2001, respectively. In 2000 he joined the Department of Electrical Engineering of University of Rome "La Sapienza" as a Researcher in Electrical Power Systems. His main research interests are in power systems analysis, distributed generation, power quality and electromagnetic transients, long distance transmission, long HV and EHV AC cable lines. He is a member of IEEE Power and Energy Society and of AEI (Italian Electrical Association).

Marco Maccioni was born in Anagni on June 24, 1978. He received a University degree in Electrical Engineering from University of Rome "Sapienza" in 2005 and currently he is a Ph.D student in Electrical Engineering. From 2007 he is an adjunct professor of Electrotechnics at the same University. His main interests include power system analysis, non-linear electromagnetic problems related to lightning protection systems and grounding systems, as well as, non-linear coupled electro-magnetic-thermal problems solved in time domain by circuital approaches